ATMOSPHERIC BOUNDARY LAYER RESEARCH AT CABAUW

A. P. VAN ULDEN[1] and J. WIERINGA[2]
[1]*Royal Netherlands Meteorological Institute, De Bilt, The Netherlands;*
[2]*Dept. of Meteorology, Wageningen Agricultural University, The Netherlands*

(Received in final form 19 October, 1995)

Abstract. At Cabauw, The Netherlands, a 213 m high mast specifically built for meteorological research has been operational since 1973. Its site, construction, instrumentation and observation programs are reviewed. Regarding analysis of the boundary layer at Cabauw, the following subjects are discussed:

- terrain roughness;
- Monin–Obukhov theory in practice;
- the structure of stable boundary layers;
- observed evolution of fog layers;
- inversion rise and early morning entrainment;
- use of the geostrophic wind as a predictor for wind profiles;
- height variation of wind climate statistics;
- air pollution applications: long range transport and short range dispersion;
- dependence of sound wave propagation on boundary-layer structure;
- testing of weather and climate models.

1. Facts about Cabauw

In this section we review briefly the history, site, mast and observation programs of the Cabauw observation facility.

1.1. Short history of the Cabauw mast

Activities of the Royal Netherlands Meteorological Institute (KNMI) are not only directed to weather forecasting and descriptive climatology of land and sea, but also deal with applications in e.g. aeronautics, hydrology and air pollution. To this end experimental programs were set up to establish relations between the state of the atmospheric boundary layer (ABL), land surface conditions and the general weather situation for all seasons. When existing radio masts proved intractable for good observations, a mast building program was started. First an 80 m mast was built in Vlaardingen, in the middle of a heavily industrialized area (Rijkoort *et al.*, 1970). This pilot project was useful, both to obtain some local pollution climatology and to gain experience in the practical problems of mast measurements. The Vlaardingen mast was dismantled in 1972, having become unsafe due to pollution erosion.

With respect to instrumentation, KNMI had also developed useful expertise with its weather station network and during the organization of large evaporation experiments at Rottegat and at Lake Flevo (see Wieringa, 1972; Keijman, 1974; and De Bruin, 1982). Much of the instrumentation was developed and built in-house, because commercially available instruments were often not good enough

Boundary-Layer Meteorology **78:** 39–69, 1996.

(e.g. not able to measure wind speeds at below 3 m s^{-1}, or not able to work well in our humid climate).

Having this experience, KNMI was well prepared to undertake the design and construction of the mast in Cabauw. Measurements started in December 1972. With some interruptions, these measurements have gone on until the present time.

1.2. The Cabauw Site

The Cabauw mast is located in the western part of the Netherlands (51.971 °N, 4.927 °E). This site was chosen, because it is rather representative for this part of the Netherlands and because only minor landscape developments were planned in this region. Indeed the present surroundings of Cabauw do not differ significantly from those in 1973. The North Sea is more than 50 km away to the WNW, and there are no urban agglomerations within 15 km radius. The nearby region is agricultural, and surface elevation changes are at most a few metres over 20 km. Within 40 km radius there are four major synoptic weather stations, among which is the regular radiosonde station at De Bilt, ensuring a permanent supporting mesoscale network.

Near the mast, the terrain is open pasture for at least 400 m in all directions, and in the WSW direction for 2 km (Figure 1). Farther away, the landscape is generally very open in the West sector, while the distant East sector is rather rough (windbreaks, orchards, low houses). The distant North and South sectors are mixed landscapes, much pasture and some windbreaks. So the highest mast levels have in all directions a long fetch of landscape roughness which is usefully similar to the roughness observed in the lower surface layer (Wieringa, 1989). An effective all-azimuth mesoscale roughness length of $z_0 \approx 0.15$ m matches well with observed ABL behaviour. Sectorwise roughness lengths are given by Van Ulden *et al.* (1976) and by Beljaars and Holtslag (1991). Panoramic photos from the top of the mast are shown by Driedonks (1981).

On the mast itself no undisturbed measurements can be made below 20 m. Auxiliary 20 m masts are installed to the SE and the NW at sufficient distance from the mast foot building. South of the mast is a well-kept observation field for micrometeorological observations, including soil heat flux, soil temperatures and various radiation measurements; north of the mast is a spare observation field. The soil consists of 0.6m of river-clay, overlying a thick layer of peat; its structure has been investigated in some detail (Jager *et al.*, 1976). The water table is about 1 m below the surface, but can be higher during wet periods.

1.3. The Cabauw Mast

The Cabauw mast was specifically designed and built as a flexible observation platform for boundary-layer research and air pollution studies. The mast is a closed cylinder of 2 m diameter, with an elevator inside. It is guyed at four levels, and carries booms at 20 m intervals in three directions (Figure 2). The 9.4 m booms

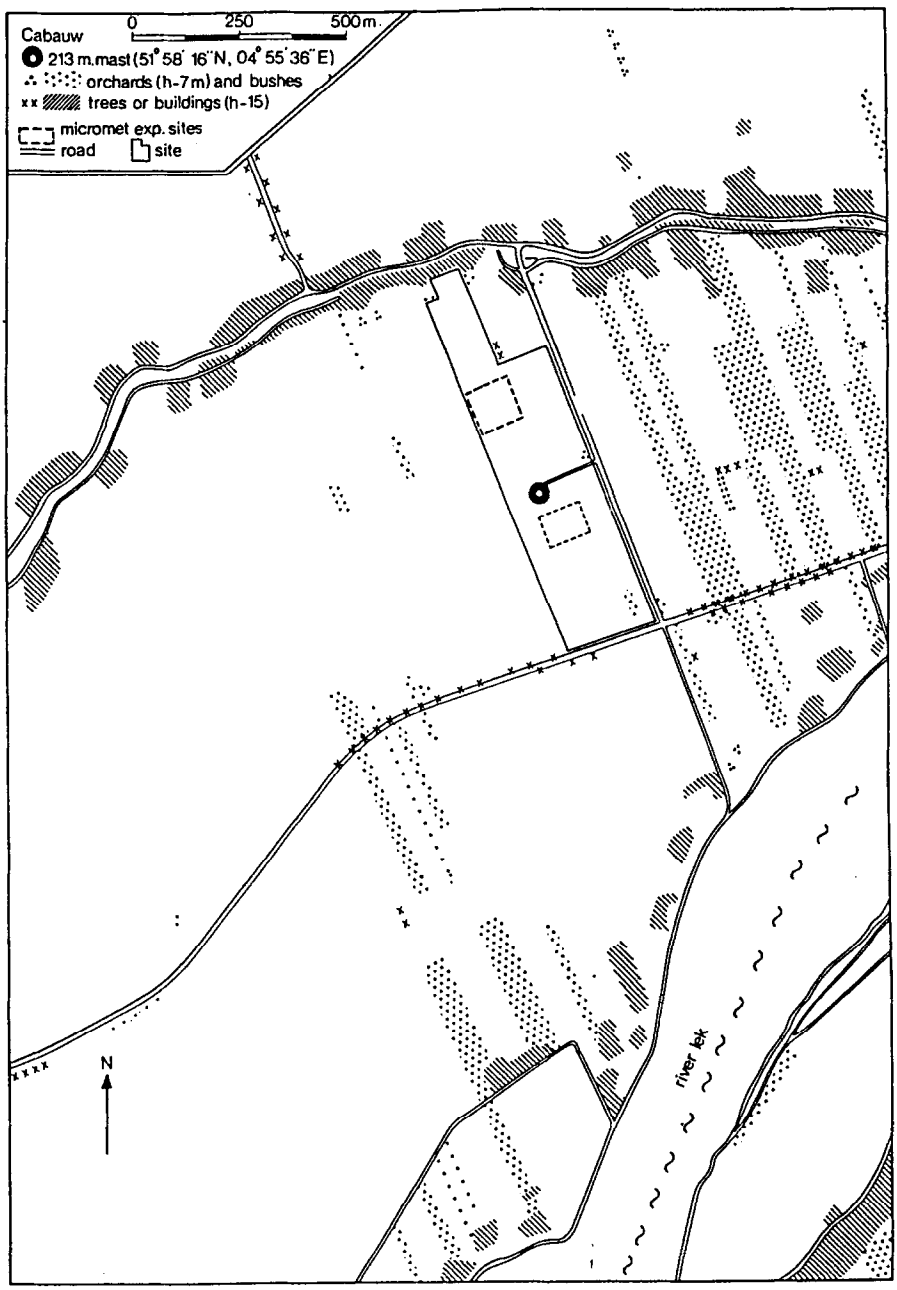

Figure 1. Local map of the site of the Cabauw mast, showing terrain characteristics. White indicates pasture.

Figure 2. Raising a boom on the Cabauw mast.

can be swung up hydraulically, so that instruments at their ends can be handled from an upper balcony; this swivelling mounting allows much longer booms than the customary sideways-sliding construction. Permanent signal cables in the boom tubes run through the hollow swivel axis, so during boom motion they are only torsion-deformed, a more endurable load than bending. Built around the mast foot is a 200 m^2 streamlined building for registration and mainenance use.

Though the booms are long enough to reduce flow interference by the mast to about 1% at the upwind side (Gill *et al.*, 1967), the boom construction itself also disturbs airflow. Comparative experiments in 1974 have shown that it was

necessary to place the actual sensor head at least 0.8 m above the slender boom end construction in order to get flow deviations which could be routinely corrected, to $\pm 1\%$ for velocity and $\pm 1°$ for azimuth (Van der Vliet, 1981; Wessels, 1984a).

Obstruction is only a problem for wind observation. Slob (1978) proved experimentally that average temperatures at the ends of upwind and downwind booms differed by less than 0.05 K. He also found that insulated radiation shields and a ventilation speed of ≈ 8 m s^{-1} were necessary to attain this ± 0.05 K accuracy. If ventilation speeds were much less than ambient wind speed, heat transfer between sensor and shield occurred due to internal circulations. In order to allow ventilated temperature observation without the necessity of placing a flow-obstructing pump at the boom's end, the lower boom tube is used as a duct for a large ventilator mounted on the mast balcony.

The long booms have another advantage. They create a unique facility to mount transmissometers with a horizontal path length of 10.5 m, allowing mast profile observation of fogs with visibilities of 500 m or less (Wessels, 1985).

For special projects, additional instruments are easily installed, since each boom has 60 signal channels as a standard. In particular, direct observations of turbulent momentum and heat fluxes have been made in many campaigns by means of all-weather propeller bivanes (Wieringa, 1972; Monna and Driedonks, 1979) combined with fast-response psychrometers (Kohsiek and Monna, 1980). For flux observations below 20 m, sonic anemometers are used instead of propeller bivanes (Schotanus, 1983). At present, mast measurements of turbulence with double-propeller K-vanes are in preparation (Bottema, 1995). More details on observations and their location, on the used instrument types and on dedicated instrumentation development, can be found in Monna and Van der Vliet (1987) and in numerous technical reports listed by Driedonks (1985).

1.4. Observation programs and data management

In the first Cabauw year, 1973, only a limited observation program was possible: wind at 10, 80 and 200 m only, with temperature at 8 levels. Half-hourly profiles over that first year were published fully (Van Ulden *et al.*, 1976). In the autumn of 1973 the number of wind observations was temporarily extended. A much enlarged program (Driedonks *et al.*, 1978) was run continuously from March 1977 to March 1979, during which period several special experiments were organized with direct observations of turbulent fluxes, balloon soundings, pollution tracer experiments, and so on. A well-checked database has been built up for these two years (Wessels, 1984b), and the run evaluations of e.g. fluxes are listed at length in several publications (see Driedonks, 1981; Nieuwstadt, 1981a; Hofman, 1988).

After some maintenance interruptions, the instrumentation was then thoroughly modernized. The observation program which has been in force since 1986 is described at length by Monna and Van der Vliet (1987) and is summarized in Table I.

Table I
Cabauw regular observation program since 1986

Height (m)	Temperatures	Wind	Visibility	Pollution	Extra measurements
200	×	×		×	
180			×		
140	×	×	×		
100			×	×	
80	×	×			
60			×		
40	×	×			
20	×	×	×		
10	×	×	×		
1.5	×		×	×	Radiation (see below)
0.6	×				

Temperatures = dry-bulb and wet-bulb temperature differences, thermocouple-measured (±0.05 K), referenced at 0.6 m and at 200 m, ventilated at 8 m s^{-1}.
Pollution = SO_2, O_3, NO and NO_2 concentrations (observed by the State Institute for Health and Environment).
Global shortwave radiation is measured at 1.5 m and 215 m. Shortwave diffuse radiation, and shortwave and longwave net radiation, are measured at 1.5 m.
Additional regular observations; monostatic acoustic sounding, pressure, rainfall; soil temperature at 0 m, −0.02 m; soil heat flux at −0.05 m, −0.10 m; water table.

Signal transport in and around the mast is essentially analog. For data handling, a PDP11/23-plus computer with analog ports and a back-up system have been installed. Every 3 sec all channels are sampled, and every 10 minutes a data processing cycle to compute mean values and standard deviations is executed. This includes a quality check to flag suspect data, and a boom selection procedure to choose undisturbed wind sensors. Then the data are transmitted to KNMI by telephone line. A final quality check is carried out manually at KNMI. Then half-hourly averages are computed, and surface fluxes of momentum, heat and latent heat are derived from the 10-minute mean values. Finally all half-hourly and 10-minute data, including e.g. acoustic sounding information, are stored on optical disc in a database (Beljaars *et al.*, 1984; Van der Vliet, 1992).

Data measured according to the procedure described here are available from 1986 onwards. Data measured in programs that were operational before 1986 are available for the periods January 1973 – December 1973 and March 1977 – February 1979 (Wessels, 1984b). Databases for two additional full years in the period 1981 – 1984 will be prepared in the near future.

For operational purposes, selected mast observations have been made available by automatic telephone link since 1977 to the forecasters at the weather services of De Bilt and various airports.

In addition to this regular program, a new two-year intensive observation period at Cabauw has been started in October 1994 as part of the Tropospheric Energy Budget Experiment (TEBEX). This project focuses both on atmospheric boundary-layer observations and on detailed detection of clouds and radiation. In this context, several remote sensing devices have been installed at Cabauw. A combination of wind profiler and RASS, a cloud lidar and an upward looking narrow-beam infrared radiometer measure profiles of wind, temperature, turbulence and cloud characteristics over the full depth of the boundary layer and even higher up. Between mast observations and remote sensing profiles an overlap exists of about 100m. This facilitates validation of the remote sensing data and continuity of the vertical profiles.

TEBEX also comprises a cloud and radiation detection network of 10 stations and a forest site for surface flux measurements in an area of $130 \times 130\,\mathrm{km}^2$ around Cabauw (Stammes *et al.*, 1994). The database will be completed with satellite observations and data from the operational KNMI weather forecast system. Some preliminary results have been reported by Feijt *et al.* (1994).

2. The Use of Cabauw Data in Surface-Layer Research

At Cabauw a long time series of surface fluxes and profiles has been obtained. This data set has been used to develop and validate parametrizations for land-surface processes. Major results are reviewed in the following two sub-sections.

2.1. Terrain roughness

The surface roughness length z_0 and the friction velocity u_* determine the structure of the neutral atmospheric surface layer. In ideal homogeneous terrain these parameters can be determined by measuring wind speed profiles in near-neutral conditions, and by application of a logarithmic wind profile to determine u_* and z_0. In practice this approach often fails. Wind speed profiles are quite sensitive to terrain inhomogeneity over fairly long fetches, and wind speed observations have limited accuracy. So the profile method is a shaky foundation for getting representative values of z_0 and u_* in the field (Priestley, 1959; Rijkoort, 1968; Peterson *et al.*, 1978). An alternative approach is to measure the turbulent momentum flux u_*^2 directly, e.g. with an eddy-correlation method, and to use the measured u_* to determine an effective roughness length. However, at ordinary weather stations eddy-correlation (or even profile) measurements are generally not available, while on the other hand maximum wind gusts are often recorded routinely.

Commencing with the idea that the ratio of the maximum gust and the mean wind speed ("gust factor") is a measure of the intensity of turbulence, Wieringa (1973, 1976, 1977, 1980a, 1995) developed a method for estimating the friction velocity and a representative roughness length from gustiness observations during strong

winds. In this method the dependence of gust maxima on anemometry dynamics, on averaging periods and on the analog recording method was accounted for. In a rigorous analysis Beljaars (1987a) extended the "gust factor" method to digital recording procedures. The practical advantage of determining roughness from station-measured gustiness is that only a single standard anemometer is needed.

In further studies it appeared useful that the Cabauw mast is not located in "ideal" flat homogeneous terrain, but in a more ordinary and weakly inhomogeneous situation. Nieuwstadt (1978), Wieringa (1980a), Beljaars (1982, 1987b) and Beljaars *et al.* (1983) investigated in more detail the momentum fluxes observed at Cabauw from non-homogeneous terrain sectors. It was concluded that gust-obtained z_0-values are *effective* roughnesses, averaged over an upwind fetch of several kilometers. Using such z_0-values, wind data can be transformed to arbitrary height and roughness situations nearby by way of a blending height model (Wieringa 1976, 1977, 1980a, 1986). As a follow-up, Schmid and Oke (1990) used the Cabauw terrain situation to develop and check a three-dimensional footprint model to deal with fluxes over patchy terrain.

These wind structure investigations led to an unexpected secondary result. In evaluating the logarithmic wind profile, it is not trivial which value of the von Karman constant is used, either $\kappa = 0.35$ as obtained from the Kansas project, or $\kappa \approx 0.4$ as derived from most other experimental projects. Close study of the projects led to the conclusion that the Kansas value should be corrected towards $\kappa \approx 0.4$ because of upstream flow distortion by the Kansas mast (Wieringa, 1980b; Wyngaard *et al.*, 1982). This study induced new interest for instrument exposure problems (e.g. Wyngaard, 1981; Gill, 1982).

2.2. MONIN–OBUKHOV THEORY IN PRACTICE

Monin–Obukhov similarity theory provides a sound physical basis for the description of the structure of the diabatic surface layer. Semi-empirical functions have been established, which relate wind and temperature profiles to the surface fluxes of momentum and heat (see e.g. Nieuwstadt and Van Dop, 1982; and Garratt and Hicks, 1990). In addition, turbulence in the atmospheric surface layer can be conveniently described in terms of surface-layer similarity parameters. These parameters are the friction velocity u_*, the temperature scale θ_*, the Obukhov stability length L and the surface roughness length z_0. For practical applications of Monin–Obukhov theory – e.g. to describe air pollution dispersion, or for the evaluation of wind energy potentials above the observation height of routine weather stations –it is necessary to estimate the four similarity parameters in some manner.

Cabauw data have been used to devise a scheme for estimating surface-layer similarity parameters from routinely available observations of total cloud cover, mean wind and mean air temperature (Van Ulden and Holtslag, 1985). The scheme consists of simple parametrizations for net radiation, evaporation and soil heat flux, while Monin–Obukhov similarity functions over an estimated effective roughness

are applied for wind speed and temperature profiles. The kinematic heat flux $u_*\theta_*$ is found as a residue from the surface energy balance, and simultaneously u_* and L are obtained from the observed wind speed.

A number of steps proved to be crucial for the development of a satisfactory scheme. The first was the independent estimation of local effective roughness lengths, either from observed gustiness or from a visual estimate of terrain characteristics (Wieringa, 1992 and 1993). The second was the development of a simple method for the partitioning of sensible and latent heat flux (De Bruin and Holtslag, 1982). The third was the discovery of the impact on radiation estimates of sharp temperature gradients near the surface, and of the importance of the skin temperature in the upper part of vegetation (Van Ulden and Holtslag, 1983; Holtslag and Van Ulden, 1983; Holtslag and De Bruin, 1988; Beljaars and Holtslag, 1991). The latter discoveries explained the large variations in the nocturnal net radiation that were observed in Cabauw. The introduction of a skin temperature improved the closure of the observed surface energy balance considerably.

The final scheme (Van Ulden and Holtslag, 1985) has been tested thoroughly against Cabauw data and behaves well in all conditions. The most important uncertainties are introduced by the estimation of the parameter for moisture availability, and by the parametrizations of solar radiation, partly due to poor quality of cloud observations. Improved results are obtained when measurements of solar radiation are used. The entire scheme has been summarized into published software packages (Beljaars *et al.*, 1989; Beljaars and Holtslag, 1990), and this has opened the way to practical application of Monin–Obukhov similarity theory (e.g. Van Ulden, 1978 and 1992; Holtslag, 1984; Van Ulden and Holtslag, 1985; Gryning *et al.*, 1987).

3. Observed Characteristics of the Atmospheric Boundary Layer

The Cabauw mast has provided unique information on the structure of the ABL above the surface layer, in particular during the night and early morning, when the boundary-layer depth is often less than 200 m. In the following sub-sections ABL characteristics are discussed and illustrated by a number of typical cases, both for cloud free conditions and for conditions with fog and low clouds. Here some new material is presented. In parallel, major research results are briefly reviewed.

3.1. The Structure of Stable Boundary Layers

When the Cabauw mast became operational in 1973, much of our attention was focused on stable boundary layers (SBL). In surface-layer experiments, the nighttime temperature profiles in clear weather show surface inversions which have a monotonous decrease with height of the potential temperature gradient $\partial\theta/\partial z$.

Our first surprise was to find that *above* the surface layer this monotonous profile behavior only occurred in weak-wind conditions. In stronger, but still moderate,

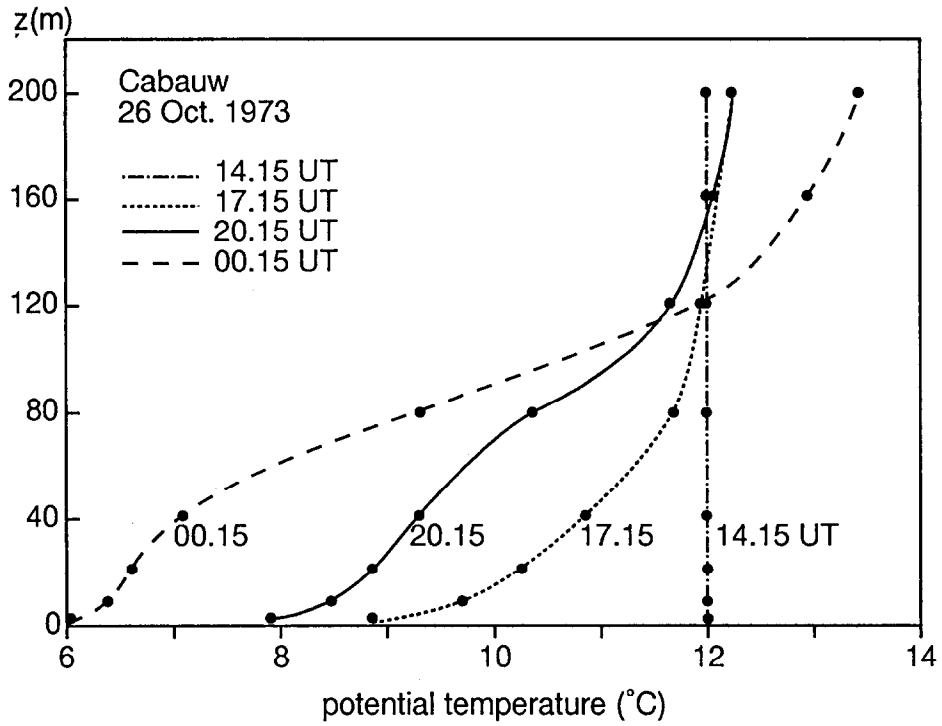

Figure 3. Observed profiles of potential temperature. Dots are observed half hourly averages. Curves are smooth interpolations. Notice the formation of an inflexion point at about 80 m.

winds we found that above the surface layer temperature gradients increased in the course of the night, leading to the formation of an inflexion point in the profiles of potential temperature. An example is given in Figure 3. The height of the profile inflexion point, below which the cooling rate is largest, appeared to increase with the windspeed at 200 m and with the geostrophic wind. Up to this height the SBL appeared to be fully turbulent. On the other hand at the top of the mast the flow was often recorded to be fully laminar.

Naturally the question was raised, what mechanism creates these structures and how is the turbulence maintained under a steadily increasing inversion strength. An answer came forth, when we added wind observations at 40 m, 120 m and 160 m to the existing observations at 10 m, 80 m and 200 m. It then appeared that often low-level jets are formed (Blackadar, 1957) with a wind maximum just above the inflexion point. Figure 4 shows an example.

In Cabauw at night, the occurrence of this type of temperature profile and low-level jet (LLJ) is more the rule than the exception. Typically the wind speed at 160 m height is greater than the wind at 200 m height for about 25% of the total time (which includes both days and nights). Similar frequent occurrences of LLJs is found over flat terrain in Poland, where the radiosonde is sent up in the early morning and reveals a consistent jet profile for clear nights (Malicki and

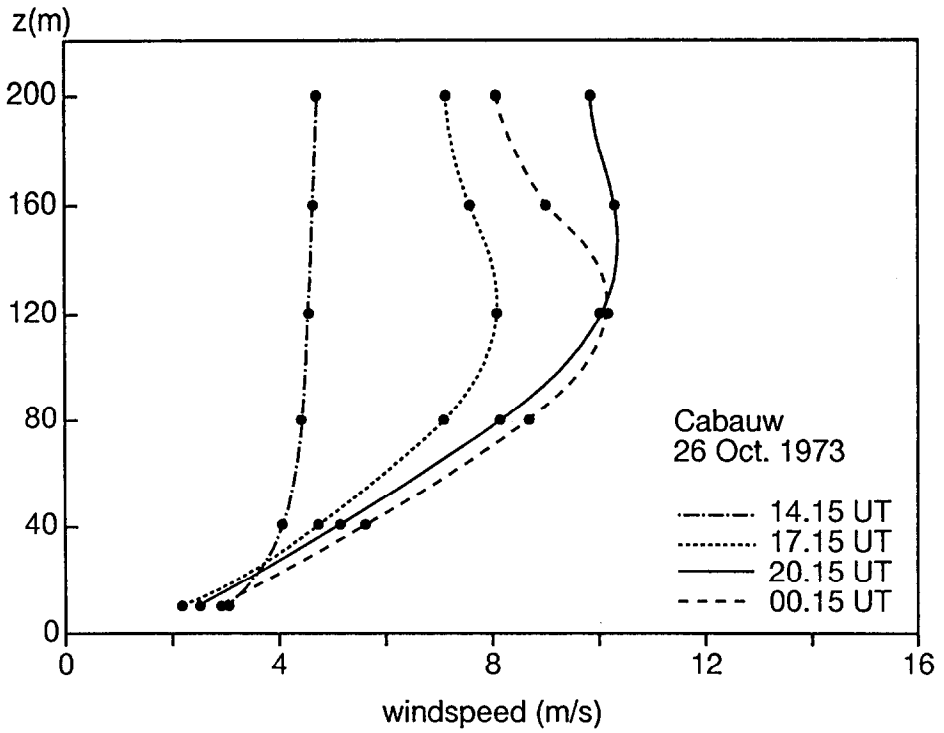

Figure 4. Observed wind speed profiles, showing development of a low level jet.

Zieleniewska, 1973). Classical studies of the low-level jet generally showed jets at several hundred meters height – but these were made in the U.S. Great Plains area, where effects of large-scale slopes are important. However, in the European plains we find that the simple Blackadar-jet is a regular feature of the ABL and *not* a insignificant side-effect, as was suggested by Lettau (1990).

Let us discuss a single case in some detail. For historical reasons we take the first jet we observed after the installation of six levels with anemometers in October 1973. The Figures 3 and 4 show the development of temperature and windspeed profiles and Figure 5 gives the corresponding hodograph for the wind vector at 200 m height. We see a characteristic example of an inertial oscillation (Blackadar, 1957). Unfortunately, a changing air mass was advected after midnight, so we did not observe a full undisturbed cycle (the inertial period in Cabauw is about 15 hours).

During the evening both the geostrophic wind and the wind at 10 m changed very little. However, the winds above the surface layer felt increasingly the influence of the inertial oscillation. The Ekman spirals became more and more curved, as is shown in Figure 6. Since the total shear includes a large directional shear contribution, it is instructive to plot vertical profiles of the integrated shear $W_E(z)$, which is defined as:

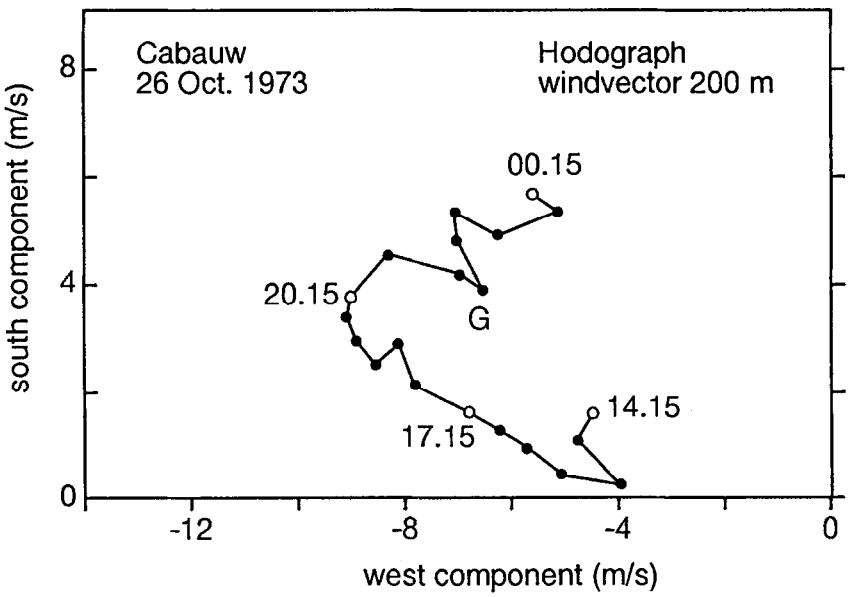

Figure 5. Hodograph of the wind vector at 200 m height. Dots and open circles are half-hourly observations. The symbol G marks the geostrophic wind, as computed according to Cats (1977). The open circles correspond with the indicated times.

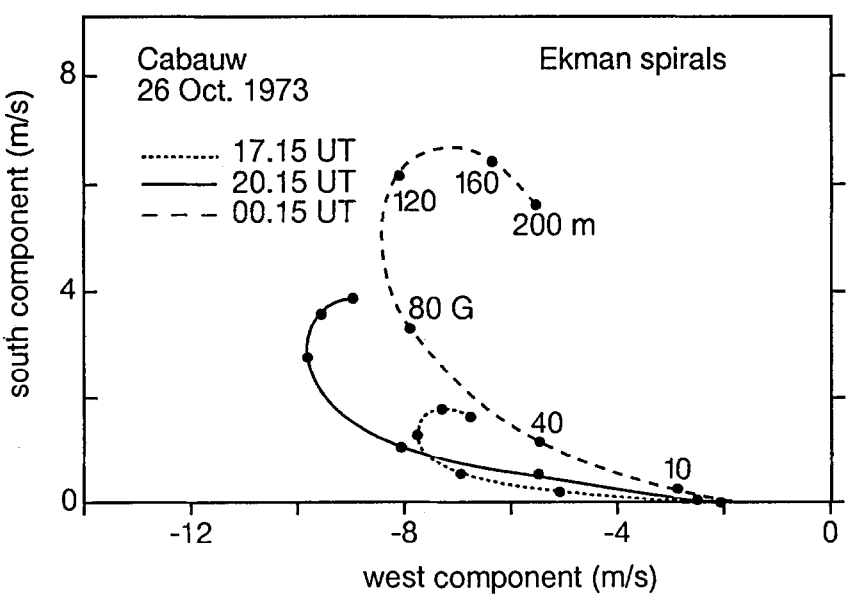

Figure 6. Evolving Ekman spirals up to 200 m. Dots are observations. The symbol G marks the geostrophic wind. Notice that the directional shear increases with time.

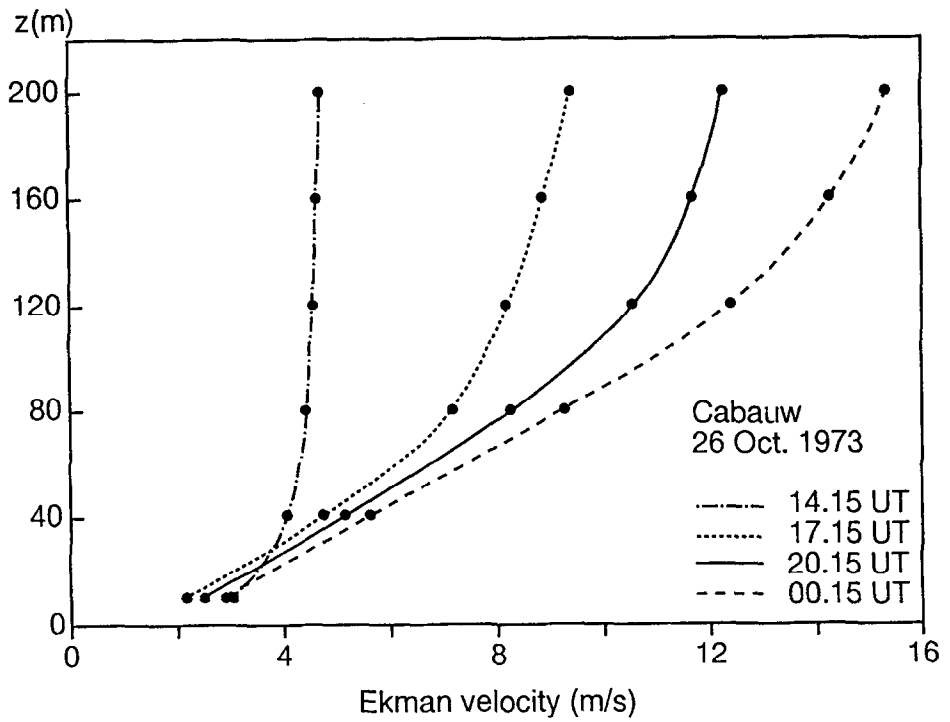

Figure 7. Profiles of the "Ekman velocity" as deduced from the Ekman spirals given in Figure 6. For definition of "Ekman velocity" see Section 3.1.

$$W_E(z) = \int_0^z |\partial \mathbf{W}/\partial z| \, \mathrm{d}z,$$

where $\mathbf{W}$ is the (complex) wind vector and where the subscript E has been used because the integrated shear is in fact the length along the Ekman spiral up to the height z. So we might call W_E the 'Ekman velocity". For the observed case W_E is shown in Figure 7. We see that, due to increasing directional shear, the integrated shear increases continually with time, even when the windspeed itself already starts to decrease at the upper levels of the mast.

From the profiles of Ekman velocity and potential temperature we can easily compute the profiles of the gradient Richardson number, defined as:

$$\mathrm{Ri} = g(\partial\theta/\partial z)/T(\partial W_E/\partial z)^2.$$

The Ri profiles are shown in Figure 8. The data at the highest level are less reliable, because of the small gradients between 200 m and 160 m. The data at the lowest level are obtained from differences between 40 m and 10 m and represent the top of the surface layer. There we find typically $\mathrm{Ri} \simeq 0.1$. In the middle of the SBL the Richardson number lies around the critical value of 0.2 used by Nieuwstadt

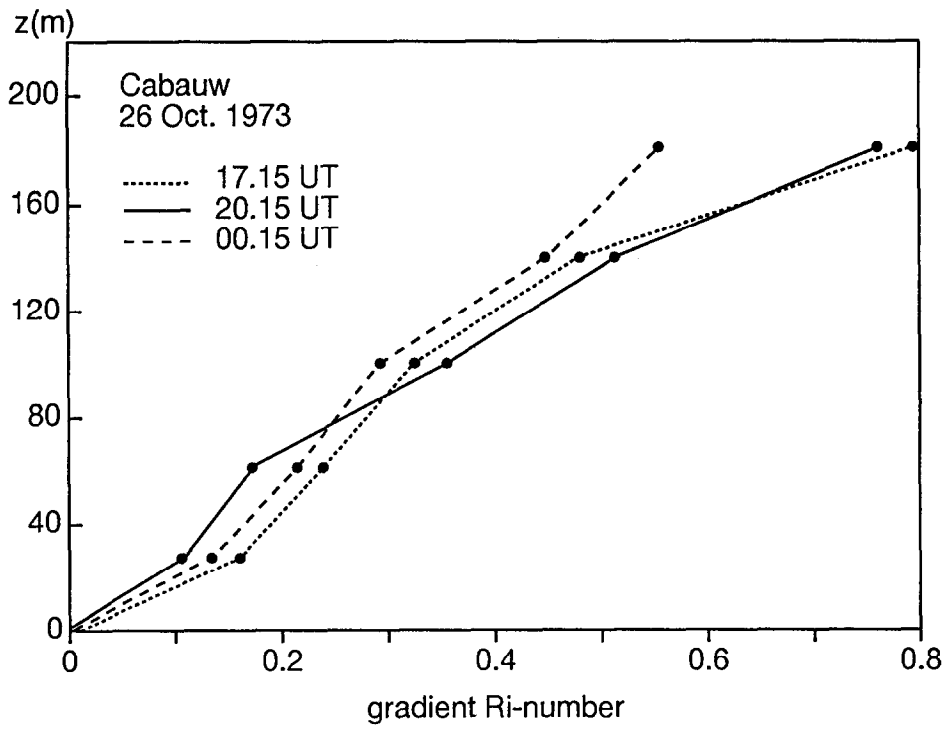

Figure 8. Profiles of the gradient Richardson number, as computed from the profiles of potential temperature and "Ekman velocity".

(1984a). This indicates that up to about 80 m there is sufficient shear to keep the SBL fully turbulent.

Another interesting feature of our data is that Ri does not seem to vary systematically with time, despite the wide range of mean profiles of wind and temperature that are involved. Apparently the internal structure of the SBL is locally in a quasi-steady state. This supports the local closure approach by Nieuwstadt (1981b, 1984a, 1984b). At the same time this analysis shows that for a full description of the SBL, time dependent inertial oscillations and radiative cooling have to be taken into account. This was done in numerical simulations of the development of the SBL in Cabauw (Tjemkes and Duynkerke, 1988; Tjemkes, 1988).

3.2. Evolution of fog layers

A unique feature of Cabauw is the measurement of light extinction at seven levels, from which profiles of visibility and fog can be deduced. In the past, fog studies have been severely hampered by lack of observations (e.g. Zdunkowski and Barr, 1972; Wessels, 1979). Cabauw data fill this gap and have been used in fog model validation (Grandin, 1983; Musson-Genon, 1987; Duynkerke, 1991) and in

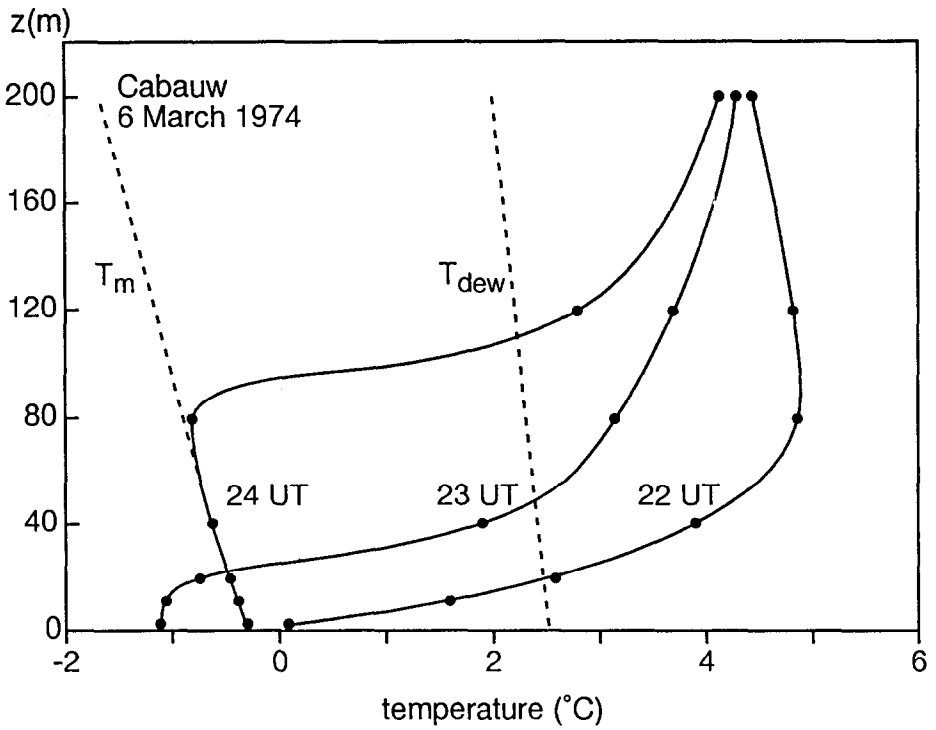

Figure 9. Fog development observed at Cabauw on 6 March 1974. Observed temperature profiles show a transition from a surface inversion to an elevated inversion. T_d marks the approximate profile of the dew point. T_m marks a moist adiabate.

phenomenological studies of fog evolution. Also, Cabauw observations are used operationally at nearby airports (Cannemeijer and Stalenhoef, 1977). Hereafter, we summarise briefly what we have learned from Cabauw observations.

Fog is a regular feature of the climate in Cabauw and many cases of fog evolution have been observed. Usually fog is formed by radiative cooling during clear nights. The resulting stable stratification obstructs turbulent exchange in the surface layer, and when wind speeds are low (say < 2 m s^{-1}) only shallow ground-fog develops. These ground fogs have the largest density close to the ground with tops below about 20 m. At very low wind speeds, dewfall occurs instead of ground fog (e.g. Holtslag and De Bruin, 1988).

When wind speeds are higher than about 2 m s^{-1} a different evolution is observed. Then enhanced turbulent mixing leads to the cooling of a deeper layer. As the ground fog grows, both in density and height, an increasing number of fog droplets will be absorbing and emitting radiation. By the time "the sky becomes invisible" (in WMO-jargon), surface cooling by upward radiation is fully compensated by downward radiation from the fog droplets. The top of the fog layer then becomes the active cooling surface, and stratification in the fog-layer changes from

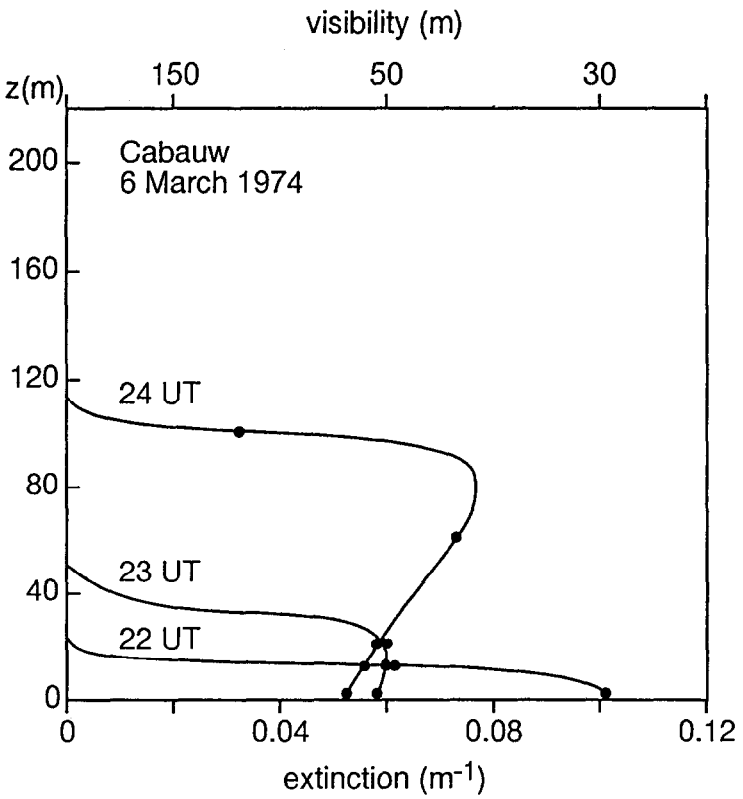

Figure 10. Fog development observed at Cabauw on 6 March 1974. Shown are profiles of the observed extinction E and the computed visibility Vis, using Vis = $3.0/E$ (Wessels, 1972). The liquid water content of fog ρ_l can also be estimated, using $\rho_l = c_l r_m E$, where $c_l = 660$ kg m^{-3} and r_m is the radius (in m) of the droplets which contribute most to the liquid water content. Typically $r_m \simeq 10^{-5}$ m for this type of fog (Wessels, 1972). Thus at 24 UT the liquid water content at 80 m height is about 0.5 g m^{-3} for this case.

stable to slightly unstable. At Cabauw, this transition from "young" ground-fog to "mature" layer-fog generally requires a fog-layer thickness of about 50 m. During transition, fog-layer mixing makes the surface temperature rise, which improves visibility near the surface. Also mixing of momentum is enhanced, which affects the surface wind. After transition, the densest fog is found just below the layer top, where a sharp temperature-inversion is present and where often significant wind shear is observed. A typical example of the transition of young ground fog to mature layer fog is shown in the Figures 9 and 10.

Another example of fog evolution is shown in Figure 11. This figure shows not only the development during the night, but also the early morning evolution. After sunrise, the fog starts dissolving from below and is 'lifted' to become stratocumulus. This feature is explained by the fact that after sunrise longwave radiative cooling still exceeds shortwave absorption at the fog-layer top, while the solar radiation

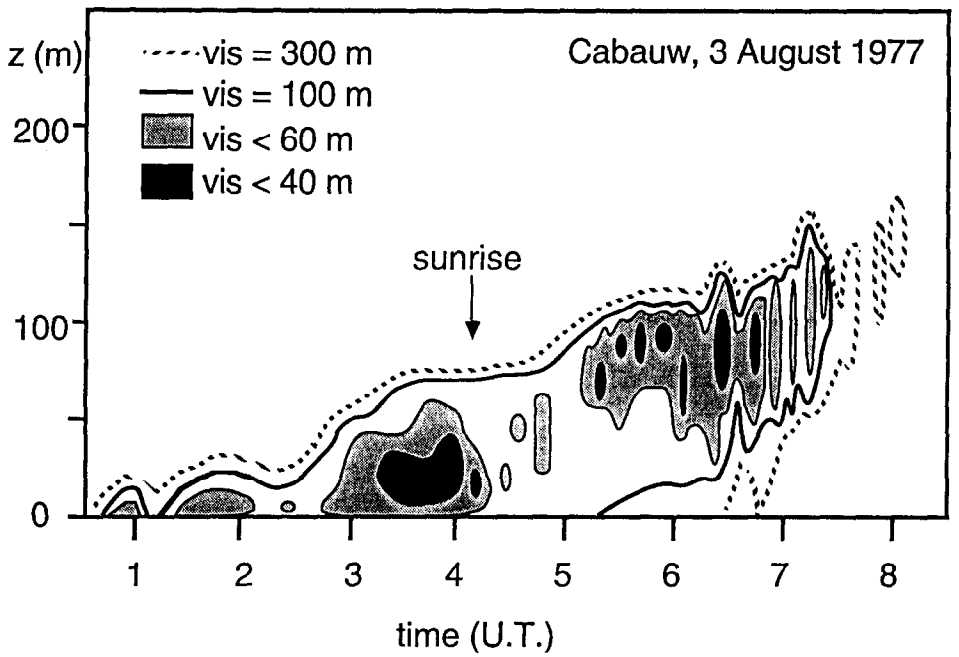

Figure 11. Fog evolution observed at Cabauw on 3 August 1977. Shown are isolines of visibility (Vis) as computed from the observed extinction (Wessels, 1972). Notice the fog lifting and break up after sunrise. See Section 3.2 for further explanation.

which passes through the fog layer assists in heating the ground. Thus the mixed fog layer is warmed and dissolved from below by the turbulent heat flux from the irradiated ground. In addition, surface heating and fog-top cooling create convective motions in the fog layer, which give rise to the formation of stratocumulus and to entrainment of dry warm air from above. This enhances the evaporation of the remaining liquid water.

3.3. Inversion Rise and Early Morning Entrainment

Inversion rise research at KNMI started in October 1971, when KNMI was asked to analyse a severe smog episode in the Netherlands (Van Ulden *et al.*, 1971). Downward mixing of accumulated pollution (fumigation) appeared to have played a major role in this episode. A forecast procedure was developed which was based on a simple encroachment model and a simple operational parametrization for the heat flux, mainly based on solar elevation.

A more sophisticated approach was introduced by Tennekes (1973b), who proposed a slab model and a closed set of equations for the inversion height h_i, the inversion strength (i.e. the temperature jump $\Delta\theta$ at the inversion) and the potential

temperature θ_m of the mixed layer. His original equation for the inversion height can be written as:

$$dh_i/dt = c_f H_0/\rho c_p \Delta\theta + c_s u_*/\mathrm{Ri}_*,$$

where H_0 is the surface heat flux, $\mathrm{Ri}_* = g h_i \Delta\theta/\theta_m u_*^2$ a turbulent bulk Richardson number and c_f, c_s are empirical coefficients. The heat flux term in this equation gives the contribution of convective turbulence to the entrainment rate (dh_i/dt) and the last term is the contribution of turbulence produced by wind shear (Kato and Phillips, 1969).

The first validation of the Tennekes model was made by Tennekes and Van Ulden (1974). In their study the earlier mentioned simple operational heat flux estimation method was applied to radiosonde data from De Bilt. In addition 10 days were analysed in some detail, using Cabauw profiles as initial condition and measured radiation for estimating the heat flux. Since this study focused on forecasting mid-day conditions, the shear term was neglected in the entrainment equation. For the convective entrainment coefficient $c_f \cong 0.2 - 0.5$ was found. The model performed well, and it was used for the development of an operational weather forecast model in which the boundary-layer development was computed along air mass trajectories (Reiff *et al.*, 1984).

More detailed studies on inversion rise were performed in the late seventies (Driedonks, 1981, 1982a, 1982b; Tennekes and Driedonks, 1981; Driedonks and Tennekes, 1984). For these studies special measurement campaigns were carried out at Cabauw with turbulent flux measurements and frequent releases of radiosondes. Moreover, measurements with an acoustic sounder were used for the detection of inversion rise. With this material the entrainment model was refined and thoroughly tested.

In all these studies the Cabauw profiles were only used to provide initial conditions. This was unfortunate, because the Cabauw profiles are ideally suited to test the shear term in the entrainment equation, since in the early morning the inversion height often remains below 200 m for several hours. Moreover at this time of the day the heat flux contribution to the entrainment is negligible in comparison with the shear term.

Thus it makes sense to re-analyse the Cabauw cases used by Tennekes and Van Ulden (1974), as well as a few other cases. In this analysis, 4-minute running means have been used, because temperature profiles change so rapidly during the night-day transition, that standard half-hourly averages would smooth the profiles too much. Each analysis starts at the moment $\partial\theta/\partial z$ vanishes near the surface. Temperature profiles have been interpolated by hand and the inversion height and inversion strength are determined as illustrated in Figure 12. This yields time series of h_i and $h_i\Delta\theta$. From these, the time rate of change $\delta h_i/\delta t$ of the inversion height in a time interval δt is found from the linear trend, while for $h_i\Delta\theta$ the average value is computed. The friction velocity is determined from the 10 m wind in the same

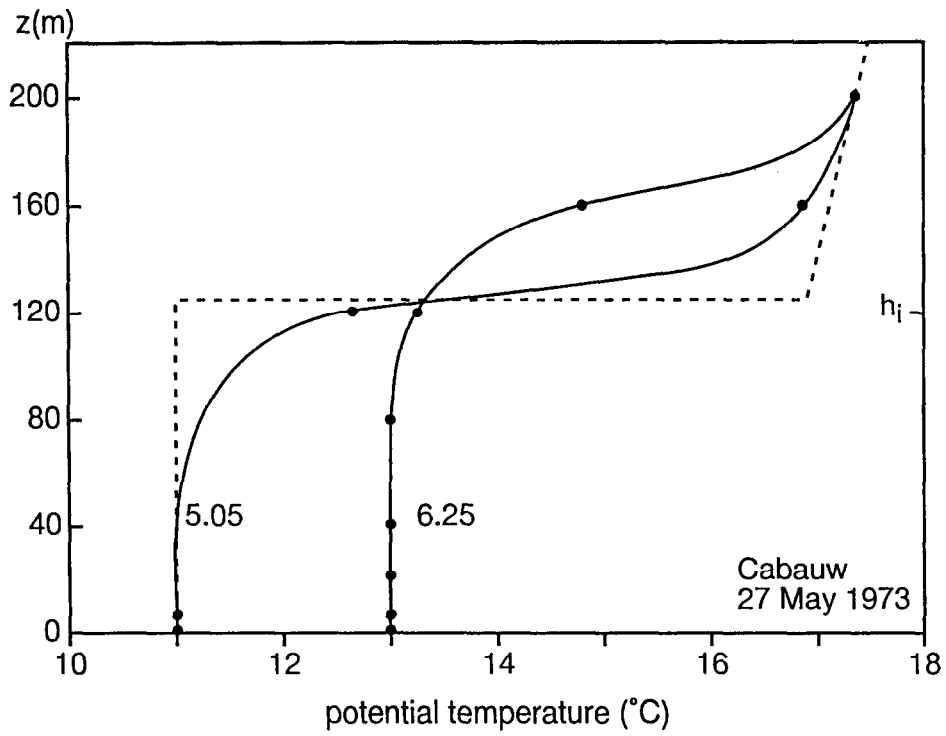

Figure 12. Example of early morning entrainment, showing two characteristic profiles of potential temperature and the slab-model representation of the first profile. Take note of the cooling in the entrainment zone.

time interval by using the roughness appropriate to the wind direction. Relevant data are given in Table II.

For the entrainment coefficient, an average value $c_s = 3.6$ is found. This value falls nicely in the range (2.5–5.0) found by Kantha *et al.* (1977) from laboratory data and by Driedonks (1982b). In Figure 13 the model with $c_s = 3.6$ is compared with the observations.

4. Wind climate studies

With the long time-series of wind profiles observed in Cabauw, various wind climate studies have been made. In the first place surface-layer similarity theory has been used to describe the wind above the surface layer. It appeared that this approach has a significant skill up to 200 m, even when the stability is estimated from routine weather data (Holtslag, 1984; Van Ulden and Holtslag, 1985; see also Section 2.2). Next geostrophic similarity theory has been evaluated. This work is described in Section 4.1. Finally a statistical approach using Weibull distributions is described in Section 4.2.

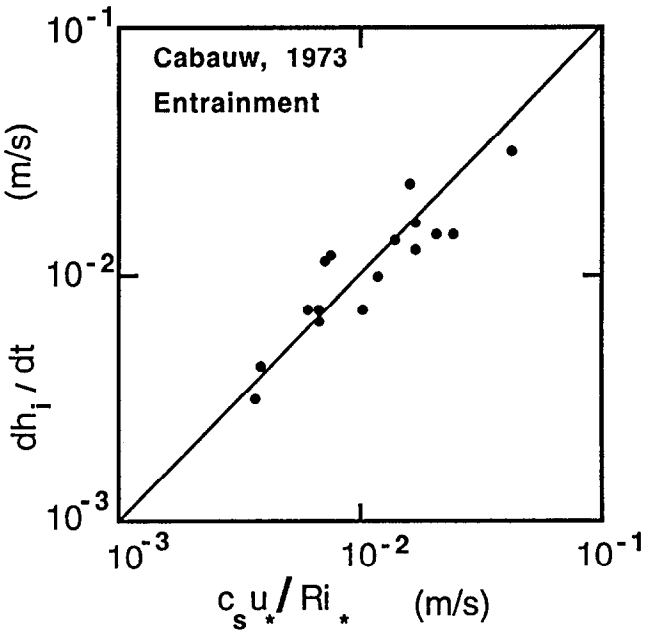

Figure 13. Comparison of observed early morning entrainment (dh_i/dt) and modelled entrainment ($c_s u_*/\mathrm{Ri}_*$, with $c_s = 3.6$). The data are specified in Table II.

Table II

Early morning entrainment at Cabauw in 1973

Date	δt (s)	δh_i (m)	$h_i \Delta\theta$ (m K)	u_* (m s^{-1})	Ri_*	c_s
March 22	5000	34	240	0.24	144	4.1
March 23	5000	33	173	0.22	124	3.7
March 24	5000	52	626	0.35	177	5.3
April 22	3600	51	388	0.44	69	2.2
April 28a	3600	34	199	0.28	88	3.0
April 28b	3600	52	217	0.34	65	2.8
April 30	3600	116	407	0.54	48	2.9
May 16	2400	32	121	0.25	67	3.6
May 26	5000	30	156	0.21	123	3.5
May 27	5000	35	697	0.40	151	2.6
June 12a	3600	40	197	0.24	115	5.5
June 12b	3600	80	230	0.32	78	5.4
June 22	3500	42	678	0.47	106	2.7
June 23	3500	55	556	0.44	99	3.5
July 1	3600	16	245	0.21	193	4.1
July 2	7200	24	730	0.29	300	3.4

4.1. USING THE GEOSTROPHIC WIND AS PREDICTOR FOR ABL WIND PROFILES

For the neutral ABL, geostrophic drag laws have been well established in the early seventies, both theoretically (Blackadar and Tennekes, 1968) and experimentally (e.g. Deacon, 1973). These drag laws allow an estimation of the friction velocity u_{*n} and the cross-isobar angle α_n between the surface stress and the geostrophic wind vector $\mathbf{G}$, from knowledge of the geostrophic wind, the Coriolis parameter f and the surface roughness z_0 alone. Rossby-number similarity theory predicts in addition (e.g. Tennekes, 1973a, 1982; Khakimov, 1976; Van Ulden and Holtslag, 1980), that the nondimensional ageostrophic wind components in the neutral boundary layer are universal functions of the nondimensional height $\xi = zf/u_{*n}$, i.e.:

$$(U - U_g)/u_{*n} = F_x(\xi) \quad \text{and} \quad (V - V_g)/u_{*n} = F_y(\xi).$$

Here the x-axis is taken in the direction of the surface stress, $U_g = G\cos\alpha_n$, $V_g = -G\sin\alpha_n$ and F_x and F_y are universal functions of ξ. Rossby-number similarity theory also suggests (Blackadar and Tennekes, 1968) that the nondimensional height of the neutral ABL is given by

$$\xi_n = h_n f/u_{*n} = C,$$

where h_n is the height of the neutral ABL and C is an empirical constant.

The universal functions F_x and F_y should satisfy a number of constraints (Van Ulden and Holtslag, 1980). In the first place the geostrophic drag laws should be retrieved for $\xi = \xi_0 = z_0 f/u_{*n}$, because U and V vanish at this lower boundary. In the second place F_x and F_y and their vertical derivatives should vanish at the upper boundary ξ_n. In the third place they should satisfy the logarithmic law in the inertial sublayer (where $\xi_0 \ll \xi \ll \xi_n$). In the fourth place they should satisfy the boundary conditions for the stress. This last constraint yields by vertical integration of the steady-state momentum equations:

$$\int_{\xi_0}^{\xi_n} F_x \,\mathrm{d}\xi = 0 \quad \text{and} \quad \int_{\xi_0}^{\xi_n} F_y \,\mathrm{d}\xi = 1.$$

With all these constraints, there is very little freedom left for devising a similarity function. Van Ulden and Holtslag (1980) proposed the following simple form:

$$F_x = ((1/\kappa)(\ln\xi + A + a\xi)[1 - (\xi/C)]^2 \quad \text{and}$$

$$F_y = (1/\kappa)(B + b\xi)[1 - (\xi/C)]^2,$$

where $A = 1.9$ and $B = 4.7$ are constants taken from the geostrophic drag laws (Deacon, 1973). Further we take $\xi_n = C = 0.3$. Then the values of a and b can be computed from the stress boundary conditions. These yield the following relations:

$$a = [(22/3) - 4\ln C - 4A]/C \quad \text{and} \quad b = (12\kappa - 4BC)/C^2.$$

For $A = 1.9$, $B = 4.7$ and $C = 0.3$ these equations give $a = 15$ and $b = -8$.

Van Ulden and Holtslag (1980) tested the above similarity profiles against Cabauw data for the full year 1973. Since this paper is not easily accessible, we give here a re-analysis of the main results. The geostrophic wind was computed according to Cats (1977) with a procedure based on principal component analysis of all 19 pressure stations in the Netherlands. Periods with rain or instrumental errors were excluded. It was further required that the geostrophic wind speed $G >$ 4 m s^{-1}. In all, 4400 hourly data remained. For each hour the geostrophic wind was computed, then u_{*n} and the cross-isobar angle α_n, and finally the wind components at 10 m, 80 m and 200m, taking $z_0 = 0.15$ m. The computed components were then compared with the mast observations.

First, we tested the neutral drag law for a near-neutral subset of our data. For this subset the "observed" u_* was computed from the observed wind speed at 10 m using a logarithmic profile and $z_0 = 0.15$ m. For these data the dimensionless "observation height" is $z_0 f / u_{*n}$. It should be noted that this dimensionless height varies with the magnitude of the geostrophic wind. The results are shown in the lower part of Figure 14 for three classes of the geostrophic wind. We see that Deacon's drag laws perform very nicely.

Next we tested the predictions with the similarity model against observations for the full data set and all observation heights. Thus no information on stability has been used in this comparison. Figure 14 shows the results. Plotted are averages for three classes of the geostrophic wind and for the three mast observation heights. The plotted standard errors apply to all data for a given observation height.

The comparison for the full data set shows very little bias at 200 m, where the standard error is not more than about 25% of the geostrophic wind speed. Part of this error can be explained by the occurrence of inertial oscillations and by other forms of dynamical imbalance. Apparently these features cancel on average. For the lower levels we see more bias, which can be explained from the fact that there are many more stable hours than unstable hours in a year. So at lower heights we see on average lower wind speeds and greater turning angles than predicted by the neutral similarity model. Overall, the performance of the model is surprising, in view of its simplicity.

4.2. Climatology of the Diurnal Course of Wind Profiles

The average diurnal course of surface-layer wind has a daytime maximum, but in the Ekman layer winds have an average nighttime maximum – distinctively in clear weather, less so in overcast situations. This ties in with the frequency of low-level jets discussed in Section 2.3 above. Though this wind behaviour was known in principle (Peppler, 1921; Matveev, 1967; Crawford and Hudson, 1973), only vague estimates existed of the height at which the diurnal course has its phase reversal.

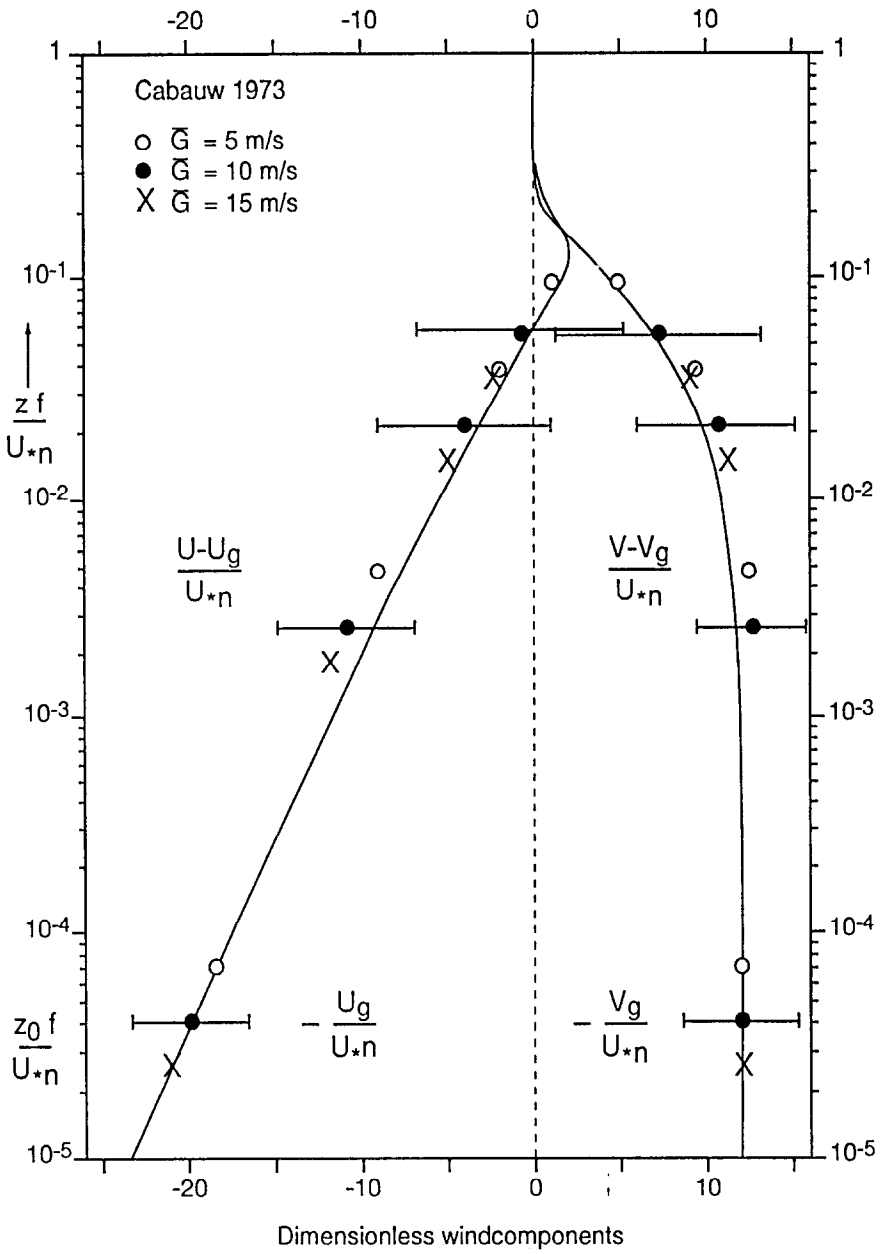

Figure 14. Dimensionless wind vector as function of the dimensionless height. Geostrophic winds were computed according to Cats (1977). The friction velocity u_{*n} and the cross-isobar angle α_n have been computed hourly from the geostrophic wind using the neutral geostrophic drag law according to Deacon (1973). The direction of the geostrophic wind and the turning angle determine the hourly orientation of the coordinate system. The real height z and the neutral height scale u_{*n}/f determine the hourly dimensionless height. Symbols give, for a full year of data, the averages of the observed scaled variables for 3 classes of the geostrophic wind speed and for the observation heights 10 m, 80 m and 200 m. Bars denote standard deviations. Curves present the similarity model proposed by Van Ulden and Holtslag (1980). The data plotted at the dimensionless height $z_0 u_{*n}/f$ compare a near-neutral subset of surface observations with the geostrophic drag law.

A novel climatological approach was based on the inverse relation between the seasonal standard deviation of hourly average wind and the width of the seasonal wind frequency distribution, as characterized by its Weibull-distribution shape parameter k (Wieringa, 1989). Using data from Cabauw and a few other masts, it was found that the diurnal wind phase reversal height is 70 m to 90 m for non-complex land locations. Below the reversal height, a linear variation with height of the Weibull shape parameter k represents k-profiles measured on different masts significantly better than the k-z power law of Justus and Mikhail (1976). The study led to a redesign of the profile model for wind distributions used in the European wind atlas (Troen and Petersen, 1989).

5. Other Applications of Cabauw Data

In the following sub-sections we describe a number of other applications. First air pollution studies are reviewed, then the propagation of sound and last but not least the testing of weather and climate models.

5.1. Air pollution studies

Since the beginning of operations, profiles of air pollution concentrations have been measured at Cabauw by RIVM (State Institute for Health and Environment; Rijksinstituut voor Volksgezondheid en Milieu). These profiles appeared to be as interesting as those of meteorological variables.

The SO_2 monitors had just been installed, when during the late night of 18 December 1972 a very pronounced SO_2 maximum was observed at 100 m. While at the surface a fairly normal concentration of 40 μg m^{-3} was observed, the concentration at 100 m amounted to 780 μg m^{-3}, and at 200 m it was still 370 μg m^{-3}. These profiles could be explained by advection of polluted air from Germany. Since along the actual trajectory no significant local sources of SO_2 were present, the turbulent surface layer of about 60 m depth became depleted of SO_2 by dry deposition. The air aloft, however, was transported almost undiluted by a laminar low-level jet. It appeared later that low-level jets frequently act as efficient highways for the transport of air pollutants. This leads to nighttime maxima at the top of the mast, while fumigation causes morning maxima at the surface (Van Dop *et al.*, 1980). Figure 15 shows that this sequence is a regularly occurring phenomenon.

In addition to these continous measurements, dedicated dispersion experiments have been carried out in Cabauw (Nieuwstadt and Van Duuren, 1979). Here the Cabauw mast proved useful to characterize the specific dispersion conditions. In general air pollution research has benefited greatly from Cabauw research through improved characterizations of the state of the boundary layer, as is shown in reviews by Holtslag and Nieuwstadt (1986) and Gryning *et al.* (1987).

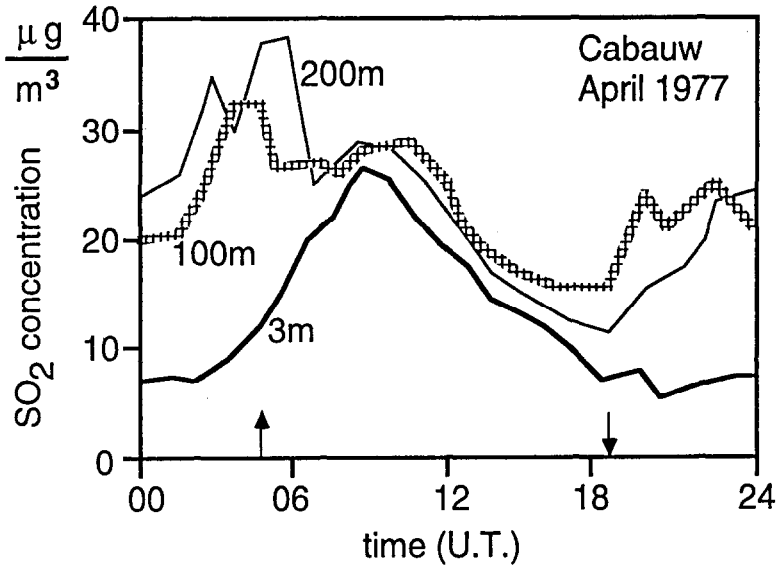

Figure 15. Diurnal variation of the SO_2 concentrations ($\mu g\ m^{-3}$), observed at Cabauw. Shown are averages over April 1977 for the heights 3 m, 100 m and 200 m. (Van Dop *et al.*, 1980). The arrows mark the time of sunrise and sunset.

5.2. Sound Propagation

The horizontal propagation of sound in the atmosphere depends on the vertical profiles of temperature and wind speed. When the sound velocity increases with height, sound rays are refracted downward and pass over obstructions such as a sound barrier along a noisy highway. In the opposite case, zones of decreased audibility may occur at some distance.

Using the 1973 Cabauw data, Wessels and Velds (1983) have calculated frequencies of occurrence of strong downward bending of sound rays. They find that in about 10% of the nights, with little dependence on season, the effect is such that sound walls of 10 m height or even larger are ineffective. Their model allows more detailed investigations of compliance with noise regulations.

Wave propagation is also affected by the spectra of temperature and humidity fluctuations. A Cabauw-based study on this issue was made by Kohsiek (1984).

5.3. Testing of Weather and Climate Models

With a high mast profiles can be measured continuously and with a great variety of accurate instruments. This allows both operational real-time use, as well as the collection of climatological data bases and the detection of rare events. A disadvantage is that a high mast is tied to a single location. In this paper we have shown that mast observations do provide information and insight that have

much wider applicability than the local characterization of the boundary layer. This explains why a new application of mast observations is increasingly acknowledged: the validation of weather and climate models.

Weather and climate models use similarity profiles for wind, temperature and humidity to connect the lowest atmospheric model level to the properties of the underlying land surface. They also employ turbulence closure schemes, soil transport equations, radiative transport equations, evaporation models, etc. All these features require careful validation and tuning, and a long time series of comprehensive data with all year representativeness. Cabauw data series are increasingly used to do such validations (Holtslag and Van Westrhenen, 1989; Beljaars and Holtslag, 1991; Holtslag and Boville, 1993; Beljaars and Viterbo, 1994; Holtslag *et al.*, 1995). Cabauw data are currently used in several international validation studies, such as the ECMWF Re-Analysis Project (ERA), and the recently-started PILPS (Project for Intercomparison of Landsurface Parameterization Schemes; see Henderson-Sellers *et al.*, 1995).

For the new observation programme TEBEX, major goals are the validation of ground based and space based remote sensing and the validation of large-scale models. This offers bright perspectives for future research with Cabauw observations.

Acknowledgements

This meteorological mast project was started in 1964 by the KNMI directors W. Bleeker and F. H. Schmidt and achieved under the responsibility of M. W. F. Schregardus. Development of the mast design was coordinated by C. M. Wierda, P. J. Rijkoort and J. Wieringa, aided by W. Auer and H. Kok of the Governmental Building Department. The construction and instrumentation were supervised by T. S. Andringa and E. P. F. H. Blokhuis.

Running the large meteorological outdoors laboratory at Cabauw requires teamwork. Particular scientific responsibility has been carried by A. C. M. Beljaars, H. A. R. De Bruin, A. G. M. Driedonks, H. Tennekes, A. P. Van Ulden, J. A. Wisse and H. R. A. Wessels. W. A. A. Monna and J. G. Van der Vliet have been acting as technical coordinators. Daily operations have been carried out by R. Agterberg, H. E. Carolus, C. A. Engeldal, H. J. M. Frerichs, C. Hofman, D. van der Luit, J. Muijsert, B. Oemraw, M. I. Rauw, T. B. Ridder, R. J. Slikker, P. J. M. Van der Veer and G. Van Vliet. Instrument development and technical support was taken care of by J. Bijma, J. J. M. Van Gorp, M. P. D. Jansse, W. Kohsiek, W. Oosterom, J. Rietman, S. Schoen, W. H. Slob, A. Unland and by K. H. Annema, J. P. H. Van Ameyde, R. H. Blankesteijn, W. Hovius, J. A. Koster, F. Renes, H. A. Schiks and L. G. M. Schiks. Computing support was given by J. J. M. Den Braber, O. J. Brinkhof, J. M. Koopstra, P. A. T. Nieuwendijk, A. Snijders, K. Veldhuijsen, J. C. Van Vuure and P. Zeldenrust.

References

Beljaars, A. C. M.: 1982, 'The Derivation of Fluxes from Profiles in Perturbed Areas', *Boundary-Layer Meteorol.* **24**, 35–55.

Beljaars, A. C. M.: 1987a, 'The Influence of Sampling and Filtering on Measured Wind Gusts', *J. Atmos. Oc. Techn.* **4**, 613–626.

Beljaars, A. C. M.: 1987b, 'On the Memory of Wind Standard Deviation for Upstream Roughness', *Boundary-Layer Meteorol.* **38**, 95–101.

Beljaars, A. C. M., Schotanus, P., and Nieuwstadt, F. T. M.: 1983, 'Surface Layer Similarity Under Nonuniform Fetch Conditions', *J. Clim. Appl. Meteorol.* **22**, 1800–1810.

Beljaars, A. C. M., Folkers, G. D. G., Hoenson, R. A., and Unlandt, A.: 1984, 'Inzameling en opslag van Cabauw-metingen: een systeemvoorstel', Roy. Neth. Meteorol. Inst. Tech. Rep. TR-48.

Beljaars, A. C. M. and Holtslag, A. A. M.: 1990, 'A Software Library for the Calculation of Surface Fluxes over Land and Sea', *Environ. Software* **5**, 60–68.

Beljaars, A. C. M. and Holtslag, A. A. M.: 1991, 'Flux Parameterization over Land Surfaces for Atmospheric Models', *J. Appl. Meteorol.* **30**, 327–341.

Beljaars, A. C. M., Holtslag, A. A. M., and Van Westrhenen, R. M.: 1989, 'Description of a Software Library for the Calculation of Surface Fluxes', Roy. Neth. Meteorol. Inst. Tech. Rep. TR-112.

Beljaars, A. C. M. and Viterbo, P.: 1994, 'The Sensitivity of Winter Evaporation to the Formulation of Aerodynamic Resistance in the ECMWF Model', *Boundary-Layer Meteorol.* **71**, 135–149.

Blackadar, A. K.: 1957, 'Boundary-Layer Wind Maxima and Their Significance for the Growth of Nocturnal Inversions', *Bull. Amer. Meteorol. Soc.* **38**, 283–290.

Blackadar, A. K. and Tennekes, H.: 1968, 'Asymptotic Similarity in the Barotropic Planetary Boundary Layer', *J. Atmos. Sci.* **25**, 1016–1020.

Bottema, M.: 1995, 'Calibration Study of the K-Gill Propeller Vane', Roy. Neth. Meteorol. Inst. Tech. Rep. TR-181.

Cannemeijer, F. and Stalenhoef, A. H. C.: 1977, 'Occurrence and Advection of Fog at Amsterdam Airport (Schiphol)', Roy. Neth. Meteorol. Inst. Sc. Rep. WR-77-12.

Cats, G. J.: 1977, 'Berekening van de geowind', Roy. Neth. Meteorol. Inst. Sc. Rep. WR-77-2.

Crawford, K. C. and Hudson, H. R.: 1973, 'The Diurnal Wind Variation in the Lowest 1500 ft in Central Oklahoma: June 1966 – May 1967, *J. Appl. Meteorol.* **12**, 127–132.

Deacon, E. L.: 1973, 'Geostrophic Drag Coefficients', *Boundary-Layer Meteorol.* **5**, 321–340.

De Bruin, H. A. R.: 1982, 'The Energy Balance of the Earth's Surface: A Practical Approach', Roy. Neth. Meteorol. Inst. Sc. Rep. 82-1.

De Bruin, H. A. R. and Holtslag, A. A. M.: 1982, 'A Simple Parametrization of the Surface Fluxes of Sensible and Latent Heat during Daytime, Compared with the Penman–Monteith Concept', *J. Appl. Meteorol.* **21**, 1610–1621.

Driedonks, A. G. M.: 1981, 'Dynamics of the Well-Mixed Atmospheric Boundary Layer', Roy. Neth. Meteorol. Inst. Sc. Rep. 81-2.

Driedonks, A. G. M.: 1982a, 'Sensitivity Analysis of the Equations for a Convective Mixed Layer', *Boundary-Layer Meteorol.* **22**, 475–480.

Driedonks, A. G. M.: 1982b, 'Models and Observations of the Growth of the Atmospheric Boundary Layer', *Boundary-Layer Meteorol.* **23**, 283–306.

Driedonks, A. G. M.: 1985, 'List of Publications on the 200 m Meteorological Mast at Cabauw, the Netherlands', Roy. Neth. Meteorol. Inst. Internal Rep. FM-85-6.

Driedonks, A. G. M., Van Dop, H., and Kohsiek, W.: 1978, 'Meteorological Observations on the 213 m Mast at Cabauw, in the Netherlands', *Prepr. 4th Am. Meteorol. Soc. Symp. on Meteorol. Obs. Instr.* (Denver) pp. 41–46.

Driedonks, A. G. M. and Tennekes, H.: 1984, 'Entrainment Effects in the Well-Mixed Boundary Layer', *Boundary-Layer Meteorol.* **30**, 75–105.

Duynkerke, P. G.: 1991, 'Radiation Fog: A Comparison of Model Simulation with Detailed Observations', *Mon. Wea. Rev.* **119**, 324–341.

Feijt, A. J., Van Dorland, R., Van Lammeren, A. C. A. P., Van Meijgaard, E. and Stammes, P.: 1994, 'Cloud-Radiation-Hydrological Interactions: Measuring and Modelling', Roy. Neth. Meteorol. Inst. Sc. Rep. 94-04.

Garratt, J. R. and Hicks, B. B.: 1990, 'Micrometeorological and PBL Experiments in Australia', *Boundary-Layer Meteorol.* **50**, 11–29.

Gill, G. C., Olsson, L. E., Sela, J., and Suda, M.: 1967, 'Accuracy of Wind Measurements on Towers or Stacks', *Bull. Amer. Meteorol. Soc.* **48**, 665–674.

Gill, G. C.: 1982, 'Comments on "A Revaluation of the Kansas Mast Influence on Measurements of Stress and Cup Anemometer Overspeeding" ', *J. Appl. Meteorol.* **21**, 437–440.

Grandin, G.: 1983, 'A 1-Dimensional PBL Model with a Sub-Grid Scale Condensation Scheme for Stratiform Clouds and Fog', Meteorol. Inst. Univ. Uppsala Rep. 72.

Gryning, S. E., Holtslag, A. A. M., Irwin, J. S., and Sivertsen, B.: 1987, 'Applied Dispersion Modelling Based on Meteorological Scaling Parameters', *Atmos. Envir.* **21**, 79–89.

Henderson-Sellers, A., et al.: 1995, 'The Project for Intercomparison of Land Surface Parameterization Schemes (PILPS): Phases 2 and 3', *Bull. Amer. Meteorol. Soc.* **76**, 489–503.

Hofman, C.: 1988, 'Description of the Cabauw Turbulence Dataset 1977–1979', Roy. Neth. Meteorol. Inst. Tech. Rep. TR-105.

Holtslag, A. A. M.: 1984, 'Estimates of Diabatic Wind Speed Profiles from Near-Surface Weather Observations', *Boundary-Layer Meteorol.* **29**, 225–250.

Holtslag, A. A. M. and Van Ulden, A. P.: 1983, 'A Simple Scheme for Daytime Estimates of the Surface Fluxes from Routine Weather Data', *J. Clim. Appl. Meteorol.* **22**, 517–529.

Holtslag, A. A. M. and De Bruin, H. A. R.: 1988, 'Applied Modelling of the Nighttime Surface Energy Balance over Land', *J. Appl. Meteorol.* **27**, 689–704.

Holtslag, A. A. M. and Van Westrhenen, R. M.: 1989, 'Diagnostic Derivation of Boundary Layer Parameters from the Outputs of Atmospheric Models', Roy. Neth. Meteorol. Inst. Sc. Rep. WR-89-04.

Holtslag, A. A. M. and Boville, B. A.: 1993, 'Local Versus Nonlocal Boundary-Layer Diffusion in a Global Climate Model', *J. Climate* **6**, 1825–1842.

Holtslag, A. A. M. and Nieuwstadt F. T. M.: 1986, 'Scaling the Atmospheric Boundary Layer', *Boundary-Layer Meteorol.* **36**, 201–209.

Holtslag, A. A. M., Van Meijgaard, E., and De Rooy, W. C.: 1995, 'A Comparison of Boundary Layer Diffusion Schemes in Unstable Conditions over Land', *Boundary-Layer Meteorol.* **76**, 69–95.

Jager, C. J., Nakken, T. C., and Palland, C. L.: 1976, 'Bodemkundig onderzoek van twee grasland-percelen nabij Cabauw', Report Heidemaatschappij N.V. (Arnhem, the Netherlands), March 1976.

Justus, C. G. and Mikhail, A. S.: 1976, "Height Variation of Wind Speed and Wind Distribution Statistics', *Geophys. Res. Lett.* **3**, 261–264.

Kantha, L. H., Phillips, O. M., and Azad, R. S.: 1977, 'On Turbulent Entrainment at a Stable Density Interface, *J. Fluid Mech.* **79**, 753–768.

Kato, H. and Phillips, O. M.: 1969, 'On the Penetration of a Turbulent Layer into a Stratified Fluid', *J. Fluid Mech.* **37**, 643–655.

Keijman, J. Q.: 1974, 'The Estimation of the Energy Balance of a Lake from Simple Weather Data', *Boundary-Layer Meteorol.* **7**, 399–407

Khakimov, I. R.: 1976, 'The Wind Profile and the Thickness of the Neutrally Stratified Atmospheric Boundary Layer', *Izv. Atm. Ocean. Phys.* **12**, 601–603.

Kohsiek, W.: 1984, 'Inertial Subrange Correlation between Temperature and Humidity Fluctuations in the Unstable Surface Layer above Vegetated Terrain', *Boundary-Layer Meteorol.* **29**, 211–224.

Kohsiek, W. and Monna, W. A. A.: 1980, "A Fast Response Psychrometer', Roy. Neth. Meteorol. Inst. Sc. Rep. WR-80-4.

Lettau, H.: 1990, "The O'Neill Experiment of 1953', *Boundary-Layer Meteorol.* **50**, 1–9.

Malicki, J. and Zieleniewska, E.: 1973, 'O noçnym maksimum pionowego profilu predkosci wiatru', *Wiadom. Sluzby Hydrol. Meteorol.* **9**, 43–49.

Matveev, L. T.: 1967, 'Physics of the Atmosphere', Isr. Progr. Sc. Transl., Jerusalem.

Monna, W. A. A. and Driedonks, A. G. M.: 1979, 'Experimental Data on the Dynamic Properties of Several Propeller Vanes', *J. Appl. Meteorol.* **18**, 699–702.

Monna, W. A. A. and Van der Vliet, J. G.: 1987, 'Facilities for Research and Weather Observations on the 213 m Tower at Cabauw and at Remote Locations', Roy. Neth. Meteorol. Inst. Sc. Rep. WR-87-5.

Musson-Genon, L.: 1987, 'Numerical Simulation of a Fog Event with a One-Dimensional Boundary Layer Model', *Mon. Wea. Rev.* **115**, 592–607.

Nieuwstadt, F. T. M.: 1978, "The Computation of the Friction Velocity u_* and the Temperature Scale T_* from Temperature and Wind Profiles by Least-Square Methods', *Boundary-Layer Meteorol.* **14**, 235–246.

Nieuwstadt, F. T. M.: 1981a, 'The Nocturnal Boundary Layer, Theory and Experiments', Roy. Neth. Meteorol. Inst. Sc. Rep. 81-1.

Nieuwstadt, F. T. M.: 1981b, 'The Steady-State Height and Resistance Laws of the Nocturnal Boundary Layer: Theory Compared with Cabauw Observations', *Boundary-Layer Meteorol.* **20**, 3–17.

Nieuwstadt, F. T. M.: 1984a, 'The Turbulent Structure of the Stable, Nocturnal Boundary Layer', *J. Atmos. Sci.* **41**, 2202–2216.

Nieuwstadt, F. T. M.: 1984b, 'Some Aspects of the Turbulent Stable Boundary Layer', *Boundary-Layer Meteorol.* **30**, 31–55.

Nieuwstadt, F. T. M. and Van Dop, H. (eds.): *Atmospheric Turbulence and Air Pollution Modelling*, Reidel Publishing Company, Dordrecht.

Nieuwstadt, F. T. M. and Van Duuren, H.: 1979, 'Dispersion Experiments with SF_6 from the 213 m High Meteorological Mast at Cabauw in the Netherlands', *Prepr. 4th Am. Meteorol. Soc. Symp. on Turb., Diff. and Air Poll.* Reno, Nevada, pp. 34–40.

Peppler, A.: 1921, 'Windmessungen auf dem Eilveser Funkturm', *Beitr. Phys. fr. Atm.* **9**, 114–129.

Peterson, E. W., Busch, N. E., Jensen, N. O., Højstrup, J., Kristensen, E.L. and Petersen, E. L.: 1978, 'The Effect of Local Terrain Irregularities on the Mean Wind and Turbulence Characteristics near the Ground', *Proc. Symp. Boundary-Layer Physics Applied to Air Pollution (Nörrköping), WMO-No.* **510**, 45–50.

Priestley, C. H. B.: 1959, 'Estimation of Surface Stress and Heat Flux from Profile Data', *Quart. J. Roy. Meteorol. Soc.* **85**, 415–418.

Reiff, J., Blaauboer, D., De Bruin, H. A. R., Van Ulden, A. P., and Cats, G.: 1984, 'An Air-Mass Transformation Model for Short-Range Weather Forecasting', *Mon. Wea. Rev.* **112**, 393–412.

Rijkoort, P. J.: 1968, 'The Increase of Mean Wind Speed with Height in the Surface Friction Layer', Roy. Neth. Meteorol. Inst. Med. Verh. 91.

Rijkoort, P. J., Schmidt, F. H., Velds, C. A., and Wieringa, J.: 1970, 'A Meteorological 80-m Tower near Rotterdam', *Boundary-Layer Meteorol.* **1**, 5–17.

Schmid, H. P. and Oke, T. R.: 1990, 'A Model to Estimate the Source Area Contributing to Turbulent Exchange in the Surface Layer over Patchy Terrain', *Quart. J. Roy. Meteorol. Soc.* **116**, 965–988.

Schotanus, P.: 1983, 'Turbulente fluxen in inhomogene omstandigheden', Roy. Neth. Meteorol. Inst. Sc. Rep. WR-82-3.

Slob, W. M.: 1978, 'The Accuracy of Aspiration Thermometers', Roy. Neth. Meteorol. Inst. Sc. Rep. WR-78-1.

Stammes, P., Feijt, A. J., Van Lammeren, A. C. A. P., and Prangsma, G. J.: 1994, 'TEBEX Observations of Clouds and Radiation: Potential and Limitations', Roy. Neth. Meteorol. Inst. Techn. Rep. 162.

Tennekes, H.: 1973a, 'The Logarithmic Wind Profile', *J. Atmos. Sci.* **30**, 234–238.

Tennekes, H.: 1973b, 'A Model for the Dynamics of the Inversion above a Convective Boundary Layer', *J. Atmos. Sci.* **30**, 558–567.

Tennekes, H.: 1982, 'Similarity Relations, Scaling Laws and Spectral Dynamics', in F. T. M. Nieustadt and H. Van Dop (eds.), *Atmospheric Turbulence and Air Pollution Modelling*, Reidel, Dordrecht, pp. 37–68.

Tennekes, H. and Van Ulden, A. P.: 1974, 'Short-Term Forecasts of Temperature and Mixing Height on Sunny Days', *Prepr. Symp. on Atmos. Diffusion and Air Pollution*, Santa Barbara, California, Am. Meteorol. Soc., pp. 35–40.

Tennekes, H. and Driedonks, A. G. M.: 1981, 'Basic Entrainment Relations for the Atmospheric Boundary Layer', *Boundary-Layer Meteorol.* **20**, 515–531.

Tjemkes, S. A.: 1988, 'Radiative Cooling in the Nocturnal Boundary Layer', Roy. Neth. Meteorol. Inst. Sc. Rep. WR-88-05.

Tjemkes, S. A. and Duynkerke, P. G.: 1988, 'The Nocturnal Boundary Layer: Model Calculations Compared with Observations', *J. Appl. Meteorol.* **28**, 161–175.

Troen, I. and Petersen, E. L. (eds.): 1989, 'European Wind Atlas', Risø Nation. Lab., Roskilde, Denmark.

Van der Vliet, J. G.: 1981, 'De invloed van de mast en de uithouders op de windmetingen te Cabauw', Roy. Neth. Meteorol. Inst. Sc. Rep. WR-81-4.

Van der Vliet, J. G.: 1992, 'File Description of Half Hourly Observation Records from the 213 m Mast at Cabauw since 1986', Roy. Neth. Meteorol. Inst., Internal Rep. FM-92-24.

Van Dop, H., Ridder, T. B., Den Tonkelaar, J. F., and Van Egmond, N. D.: 1980, 'Sulphur Dioxide Measurements on the 213 Metre Tower at Cabauw, the Netherlands', *Atmos. Environ.* **14**, 933–945.

Van Ulden, A. P.: 1978, 'Simple Estimates of Vertical Diffusion from Sources near the Ground', *Atmos. Environ.* **12**, 2121–2129.

Van Ulden, A. P.: 1992, 'A Surface-Layer Similarity Model for the Dispersion of a Skewed Passive Puff near the Ground', *Atmos. Environ.* **26A**, 681–692.

Van Ulden, A. P., Wisse, J. A., and Velds, C. A.: 1971, 'Meteorologische aspecten van de periode met een verhoogde mate van luchtverontreiniging (15 September – 4 October 1971)', Roy. Neth. Meteorol. Inst. Report (unpublished).

Van Ulden, A. P., Van der Vliet, J. G., and Wieringa, J.: 1976, 'Temperature and Wind Observations at Heights from 2 to 200 m at Cabauw in 1973', Roy. Neth. Meteorol. Inst. Sc. Rep. WR-76-7.

Van Ulden, A. P. and Holtslag, A. A. M.: 1980, 'The Wind at Heights between 10 m and 200 m in Comparison with the Geostrophic Wind', *Proc. Seminar on Radioactive Releases*, Risø, Denmark, C.E.C. Luxemburg, Vol. 1, pp. 83–92.

Van Ulden, A. P. and Holtslag, A. A. M.: 1983, 'The Stability of the Atmospheric Surface Layer during Nighttime', *Preprints Sixth Symposium on Turbulence and Diffusion*, Boston, Amer. Meteorol. Soc., pp. 257–260.

Van Ulden, A. P. and Holtslag, A. A. M.: 1985, 'Estimation of Atmospheric Boundary Layer Parameters for Diffusion Applications', *J. Clim. Appl. Meteorol.* **24**, 1196–1207.

Wessels, H. R. A.: 1972, 'Metingen van regendruppels te De Bilt', Roy. Neth. Meteorol. Inst. Sc. Rep. WR-72-6.

Wessels, H. R. A.: 1979, 'Growth and Disappearance of Evaporation Fog during the Transformation of a Cold Air Mass', *Quart. J. Roy. Meteorol. Soc.* **105**, 963–977.

Wessels, H. R. A.: 1984a, 'Distortion of the Wind Field by the Cabauw Meteorological Tower', *WMO Instr. Obs. Meth. Rep.* 15 (TECEMO Conf., Noordwijkerhout, Netherlands), pp. 251–255.

Wessels, H. R. A.: 1984b, 'Cabauw Meteorological Data Tapes 1973–1984: Description of Instrumentation and Data Processing for the Continuous Measurements', Roy. Neth. Meteorol. Inst. Sc. Rep. WR-84-6.

Wessels, H. R. A.: 1985, 'The Effect of Diffracted Light on Visibility Measurements with Transmissometers', Paper prepared for I.C.A.O., Roy. Neth. Meteorol. Inst., Memo FM-85-15.

Wessels, H. R. A. and Velds, C. A.: 1983, 'Sound Propagation in the Surface Layer of the Atmosphere', *J. Acoust. Soc. Am.* **74**, 275–280.

Wieringa, J.: 1972, 'Tilt Errors and Precipitation Effects in Trivane Measurements of Turbulent Fluxes over Open Water', *Boundary-Layer Meteorol.* **2**, 406–426.

Wieringa, J.: 1973, 'Gust Factors over Open Water and Built-Up Country', *Boundary-Layer Meteorol.* **3**, 424–441.

Wieringa, J.: 1976, 'An Objective Exposure Correction Method for Average Wind Speeds Measured at a Sheltered Location', *Quart. J. Roy. Meteorol. Soc.* **102**, 241–253.

Wieringa, J.: 1977, 'Wind Representativity Increase due to an Exposure Correction, Obtainable from Past Analog Wind Station Records', Proc. TECIMO Conf., WMO-No. 480, 39–44.

Wieringa, J.: 1980a, 'Representativeness of Wind Observations at Airports', *Bull. Amer. Meteorol. Soc.* **61**, 962–971.

Wieringa, J.: 1980b, 'A Revaluation of the Kansas Mast Influence on Measurements of Stress and Cup Anemometer Overspeeding', *Boundary-Layer Meteorol.* **18**, 411–430.

Wieringa, J.: 1986, 'Roughness-Dependent Geographical Interpolation of Surface Wind Speed Averages', *Quart. J. Roy. Meteorol. Soc.* **112**, 867–889.

Wieringa, J.: 1989, 'Shapes of Annual Frequency Distributions of Wind Speed Observed on High Meteorological Masts', *Boundary-Layer Meteorol.* **47**, 85–110.

Wieringa, J.: 1992, 'Updating the Davenport Roughness Classification', *J. Wind Engin. Industr. Aerodyn.* **41**, 357–368.

Wieringa, J.: 1993, 'Representative Roughness Parameters for Homogeneous Terrain', *Boundary-Layer Meteorol.* **63**, 323–363.

Wieringa, J.: 1995, 'Representativity of Extreme Wind Data', In V. P. Singh (ed.), *Hydrology of Disasters*, Kluwer, Dordrecht (in press).

Wyngaard, J. C.: 1981, 'The Effects of Probe-Induced Flow Distortion on Atmospheric Turbulence Measurements', *J. Appl. Meteorol.* **20**, 784–794.

Wyngaard, J. C., Businger, J. A., Kaimal, J. C., and Larsen, S. E.: 1982, 'Comments on "A Revaluation of the Kansas Mast Influence on Measurements of Stress and Cup Anemometer Overspeeding", with "Reply" by J. Wieringa', *Boundary-Layer Meteorol.* **22**, 245–250 and 251–255.

Zdunkowski, W. G. and Barr, A. E.: 1972, 'A Radiative-Conductive Model for the Prediction of Radiation Fog', *Boundary-Layer Meteorol.* **3**, 152–177.